

# Volumes and spin states of FeH<sub>x</sub>: Implication for the density and temperature of the Earth's core

HUA YANG<sup>1,2</sup>, JOSHUA M.R. MUIR<sup>1</sup>, AND FEIWU ZHANG<sup>1,\*†</sup>

<sup>1</sup>State Key Laboratory of Ore Deposit Geochemistry, Institute of Geochemistry, Chinese Academy of Sciences, Guiyang, 550081, China

<sup>2</sup>University of Chinese Academy of Sciences, Beijing, 100049, China

## ABSTRACT

Hydrogen is the most abundant element in the solar system and has been considered one of the main light elements in the Earth's core. The hydrogen content in the Earth's core is determined normally by matching the volume expansion caused by the incorporation of hydrogen into FeH<sub>x</sub> to the Earth's core density deficit. The magnitude of this volume expansion at the pressure (*P*) and temperature (*T*) conditions of the Earth's core is still unknown, and the effect of spin transition in FeH<sub>x</sub> at high pressure is usually ignored. In this study, we simulate the Fe spin transition, equation of state, and hydrogen-induced volume expansion in Fe-H binaries at high *P-T* conditions using density functional theory (DFT) calculations. Our results indicate that hydrogen could stabilize the magnetic properties of fcc Fe from ~10 to ~40 GPa. A volume expansion induced by hydrogen is linear with pressure except at the Fe spin transition pressure, where it collapses significantly (~30%). The fcc FeH lattice is predicted to expand at an average rate of ~1.38 and 1.07 Å<sup>3</sup> per hydrogen atom under the Earth's outer and inner core *P-T* conditions, where the hydrogen content is estimated to be ~0.54–1.10 wt% and ~0.10–0.22 wt%, respectively. These results suggest that the Earth's core may be a potentially large reservoir of water, with up to ~98 times as much as oceans of water being brought to the Earth's interior during its formation. Based on our predicted hydrogen content in the Earth's core, we propose that the presence of hydrogen would induce a relatively lower core temperature, ~300–500 K colder than it has been previously speculated.

**Keywords:** Hydrogen, iron hydride, spin transition, volume expansion, Earth's core; Physics and Chemistry of Earth's Deep Mantle and Core

## INTRODUCTION

The Earth's core comprises an iron-nickel alloy with some additional light elements such as Si, O, S, C, and H (Allègre et al. 1995; Ringwood 1984). Among these light elements, hydrogen has been proposed as an essential candidate in the Earth's core (Poirier 1994). FeH adopts a face-centered cubic (fcc) structure that can exist stably under the conditions of the Earth's core (Bazhanova et al. 2012; Kato et al. 2020). X-ray diffraction (XRD) and in situ neutron diffraction experiments are usually utilized to estimate the hydrogen content in the Earth's core with a linear relation:  $x = (V_{\text{FeH}_x} - V_{\text{Fe}}) / \Delta V_{\text{H}}$ , where *x* is hydrogen concentration,  $V_{\text{FeH}_x}$  and  $V_{\text{Fe}}$  are the unit-cell volumes of iron hydride and pure iron metal, respectively, and  $\Delta V_{\text{H}}$  is the volume expansion caused by a single-formula unit of hydrogen. The values of  $\Delta V_{\text{H}}$  in the Fe-H system are crucial for acquiring the hydrogen content of the core. Previous studies have reported values ranging from 1.8 to 2.7 Å<sup>3</sup> under relatively low *P-T* conditions ( $P = 4\text{--}82$  GPa,  $T < 2000$  K) (Ikuta et al. 2019; Kato et al. 2020; Narygina et al. 2011; Pépin et al. 2014; Sakamaki et al. 2009; Thompson et al. 2018). These values are obtained under conditions far from the Earth's core, however, and may underestimate the hydrogen content in the Earth's core. Therefore, the value of  $\Delta V_{\text{H}}$  needs to be explored under the *P-T* conditions of the Earth's core.

There is also considerable disagreement about the spin transition pressure of fcc FeH and its effect on volume and  $\Delta V_{\text{H}}$ . The volume expansion of fcc FeH<sub>x</sub> is approximately linear with pressure at low-*P-T* conditions (4–12 GPa, 750–1200 K) (Ikuta et al. 2019). However, the high-spin (HS) to low-spin (LS) transition in fcc FeH leads to a volume collapse and an anomaly in compression behavior (Kato et al. 2020), which will further affect the values of  $\Delta V_{\text{H}}$ . Therefore, the pressure-driven HS to LS transition in fcc FeH needs to be considered to properly determine the hydrogen content in the Earth's core. Narygina et al. (2011) suggested that at the pressure range of 26–47 GPa, the non-magnetic (NM) state of fcc FeH was observed in their Mössbauer spectroscopy experiments. Thompson et al. (2018) proposed that magnetic transition in fcc FeH is unlikely to occur at pressures up to 82 GPa. More recently, Kato et al. (2020) reported that the ferromagnetic (FM) to NM transition in fcc FeH happens at about 50–60 GPa based on their XRD measurements and theoretical calculations. Thus considerable discrepancies exist in predictions of where this transition occurs.

In this study, to examine the volume expansion  $\Delta V_{\text{H}}$  in iron hydride (FeH<sub>x</sub>), we employed theoretical calculations to model FeH<sub>x</sub> at high-*P-T* conditions. We calculated the volumes of FeH<sub>x</sub> as a function of pressure. The thermodynamic properties of FeH<sub>x</sub> were calculated using the lattice dynamics method with quasi-harmonic approximation. The spin transition in fcc FeH was determined to be at ~40 GPa. Before and after the spin transition point, the volume expansion induced by hydrogen is nearly linear

\* E-mail: zhangfeiwu@vip.gyig.ac.cn. Orcid 0000-0002-4979-0790

† Special collection papers can be found online at <http://www.minsocam.org/MSA/AmMin/special-collections.html>.

at both sides. Based on our  $\text{FeH}_x$  volume expansion data at the Earth's core  $P$ - $T$  conditions, the maximum hydrogen content in the Earth's core can be precisely re-estimated by comparison with its seismic model. Finally, we discuss hydrogen content in the inner and outer core and its implications for the Earth's interior density and temperature.

## METHODS

An evolutionary crystal structure prediction method (USPEX) (Lyakhov et al. 2013; Oganov et al. 2011) was used to search for stable Fe-H binaries at 100–400 GPa. We found that  $P6_3/mmc$ -Fe (hcp),  $Fm\bar{3}m$ -FeH (fcc),  $P_4/mmm$ - $\text{Fe}_3\text{H}_5$ ,  $Pm\bar{3}m$ - $\text{FeH}_3$ ,  $C2/m$ - $\text{Fe}_3\text{H}_{11}$ , and  $C2/c$ - $\text{FeH}_6$  are stable at high pressures, which is consistent with previous studies (Bazhanova et al. 2012). Some of the cell parameters and crystal structures of these stable components are shown in Online Materials<sup>1</sup> Table S1 and Figure S1, respectively. The phonon dispersion curves of these stable phases are shown in Online Materials<sup>1</sup> Figure S2, and no imaginary phonon frequencies were found for any of these phases, which indicates their dynamical stability.

All the produced Fe-H structures were then fully relaxed by density functional theory (DFT) (Kohn and Sham 1965) implemented in the Vienna Ab initio Simulation Package (VASP) (Kresse and Furthmüller 1996) within the generalized gradient approximation (GGA) (Perdew et al. 1996) and the projector-augmented wave (PAW) method (Blöchl 1994). Fe- $3p^63d^74s^1$  and H- $1s^1$  were treated as valence states. A plane wave cutoff energy of 500 eV and the Monkhorst-Pack scheme (Monkhorst and Pack 1976) with a  $\mathbf{k}$ -point grid of  $2\pi \times 0.05 \text{ \AA}^{-1}$  were found to give excellent stress tensors and structural energy convergence for the Fe-H system relaxations. The magnetic properties of Fe-H were calculated on a  $20 \times 20 \times 20$   $\mathbf{k}$ -point mesh. To determine the volume expansions and thermodynamic properties of Fe-H, molecular dynamics (MD) simulations were used for liquid phases (outer core), while lattice dynamics QHA runs for solid phases (inner core).

MD calculations were run at the gamma point with a cutoff of 500 eV, and the energy converged to within  $10^{-5}$  eV, and all runs were performed with 64 atoms in fixed cubic cells corresponding to  $\sim 135$  GPa. The simulations were calculated at 10000 K for 2 picoseconds (ps) to obtain a liquid structure. Then the cell was quenched to the target temperature of 4000 K and allowed to equilibrate for 2 ps. Finally, another 8 ps simulations were performed to determine the equilibrium volumes and lattice parameters by taking their averages over time. Time steps of the simulations were set to 1 femtosecond (fs). The Nosé thermostat was used for temperature control (Nosé 1984), and MD trajectories were implemented in the canonical ensemble ( $NVT$ :  $N$  = number of atoms,  $V$  = volume,  $T$  = temperature). Examination of root-mean-squared displacement (RMSD) was used to ensure the state remained in liquid, as shown in Online Materials<sup>1</sup> Figure S3. Note that MD calculations were performed for the most stable fcc FeH alloy only, where the free spin polarization was not included as its magnetism is completely lost under core pressure conditions (Kato et al. 2020). The volume expansion of the liquid phase was then used to estimate the H concentration of the outer core.

Theoretical phonon dispersion and thermodynamic properties of Fe-H binaries were obtained using both the PHON code (Alfè 2009) and PHONOPY package (Togo et al. 2008) with the direct force constant method. Supercells were used for structure relaxation and phonon calculations (hcp Fe with  $3 \times 3 \times 3$  of 54 atoms, fcc Fe and  $Pm\bar{3}m$ - $\text{FeH}_3$  with  $3 \times 3 \times 3$  of 108 atoms,  $Fm\bar{3}m$ -FeH and  $P_4/mmm$ - $\text{Fe}_3\text{H}_5$  with  $2 \times 2 \times 2$  of 64 atoms,  $C2/m$ - $\text{Fe}_3\text{H}_{11}$  with  $1 \times 2 \times 2$  of 112 atoms, and  $C2/c$ - $\text{FeH}_6$  with  $2 \times 1 \times 2$  of 112 atoms). The phonon spectrum was calculated by perturbing the volumes to create seven new structures and fully relaxing both the lattice shape and ionic positions. This quasi-harmonic approximation (QHA) neglects any additional anharmonic effects, but the total anharmonic contribution to the free energy ( $F_{\text{anham}}$ ) of hcp Fe at 360 GPa and 6000 K is only of the order of 60 meV/f.u. (Alfè et al. 2001). By comparing the free energies obtained from both MD and QHA studies for hcp Fe and  $Fm\bar{3}m$ -FeH systems, we calculated  $F_{\text{anham}}$  to be 33 meV/f.u. for Fe and 46 meV/f.u. for FeH at 360 GPa and 5000 K. Thus,  $F_{\text{anham}}$  of Fe-H binaries is in the same order of magnitude as that of hcp Fe, and the inclusion of anharmonic terms will not change our conclusions about the volume expansion in Fe-H binaries, even at very high temperatures.

Spin transition pressure calculations were determined by setting two spin states of iron: spin-restricted (SR) and non-spin-restricted (NSR). In the SR state, the occupation numbers for electrons with up and down spin were fixed to be equal, which indicates that the magnetic moments are constrained to be 0  $\mu_B$ . In the NSR state, the occupation numbers of every electronic orbital were varied independently for up and down spins, allowing the iron atoms to have a net magnetic moment if that corresponds to the minimum energy state (Vočadlo et al. 2002).

The strain-stress method was used to compute the elastic constants tensor under static conditions. We applied a deformation matrix to a  $(2 \times 2 \times 2)$  supercell to achieve the deformation with strain values of  $\pm 0.01$  and  $\pm 0.02$ , respectively. The resulting stress tensor was then plotted against the applied strain and fitted to second-order polynomials to evaluate the elastic constants (Karki et al. 2001). The Voigt average was used to calculate the bulk and shear elastic modulus since we applied a uniform strain to the supercell, and these were then propagated to the seismic wave velocities. More elastic calculation details are given in the Online Materials<sup>1</sup>.

## RESULTS AND DISCUSSION

### Spin transition

The magnetism of iron has a significant effect on its compression behavior, and the previously observed anomaly in volumes in  $\text{FeH}_x$  without a structural change may be caused by the iron spin transition (Kato et al. 2020). Here, we determined the spin transition in fcc FeH at a pressure range of 0–80 GPa since previous studies have suggested that the magnetic transition pressure in fcc FeH is  $\sim 26$ –60 GPa (Elsässer et al. 1998). Our calculations found that the spin transition in fcc FeH occurs at a volume of  $5.43 \text{ \AA}^3$  per atom, corresponding to the pressure of  $\sim 40$  GPa (Fig. 1a). This value is lower than the recently reported theoretical value of 50–60 GPa by Kato et al. (2020), but higher than the implied experimental value found by Narygina et al. (2011) who proposed that fcc FeH was in the NM or anti-ferromagnetic (AFM) state at 26–47 GPa, which suggests the spin transition is at a lower pressure than this range.

It should be pointed out that our value does not use a correction for correlation of the d-electrons in iron (such as DFT+U) and thus likely underestimates the spin transition pressure somewhat. Determining the exact value of the spin transition is difficult both theoretically and experimentally as the  $dH/dP$  slope of both the HS and LS phases are similar (0.272/0.261 at the spin transition pressure). This means that small variations in theoretical setup or experimental conditions could lead to large changes in the spin transition pressure, which is not well defined in reality. As one example, we found that the spin transition pressure was very sensitive to the size of the  $\mathbf{k}$ -point mesh and that we used a larger  $\mathbf{k}$ -point mesh than Kato et al. (2020), which may account for our lower spin transition pressure. When using corrections such as +U they are not strictly theoretically defined and the correction is often linked to empirical measurements. Our main conclusions about the effect of hydrogen on volume expansion and the concentration of hydrogen in the core are not affected by the location of the spin transition pressure unless these parameters are desired directly at the spin transition pressure or nearby pressures.

The spin transition in fcc and hcp Fe was also determined at high pressure. Figure 1b shows the Fe volume as a function of pressure for both fcc and hcp structures. The volume of fcc Fe collapses at the pressure of  $\sim 10$  GPa, indicating its spin transition pressure. Hcp Fe was found to be always stable in the NM state across the examined pressure range, and the volume was found to change perfectly linearly with pressure, which is consistent with previous studies (Söderlind et al. 1996).

The magnetization behavior of the hcp and dhcp phases of FeH has been reported by Kato et al. (2020), where the FM state of hcp and dhcp FeH was found to be stable down to 4.25 and  $5.15 \text{ \AA}^3/\text{atom}$ , respectively, with a pressure-induced continuous

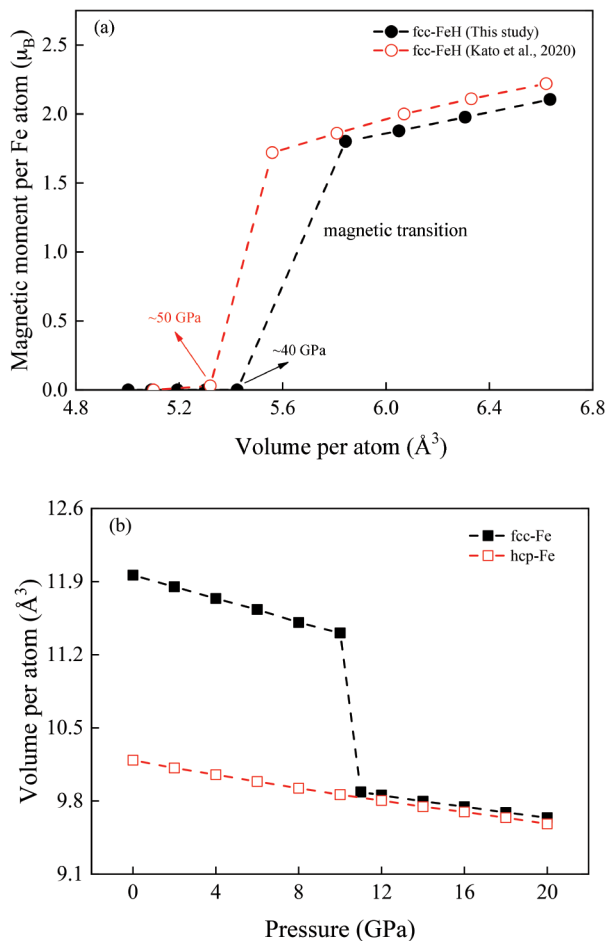


**FIGURE 1.** (a) Fe magnetic moment in fcc FeH as a function of volume. The magnetic moment of Fe collapses at the volume of  $5.4 \text{ \AA}^3$ , corresponding to the pressure of  $\sim 40 \text{ GPa}$ , comparison with  $5.3 \text{ \AA}^3$ ,  $\sim 50 \text{ GPa}$  reported by Kato et al. (2020) (red circle). (b) Volumes of fcc and hcp Fe as a function of pressure. The fcc Fe volume dropping at the pressure of  $\sim 10 \text{ GPa}$  indicates the Fe spin transition. (Color online.)

decrease in magnetic moments. This indicates that hydrogen can induce ferromagnetism in hcp Fe with pressures below  $\sim 210 \text{ GPa}$ . The volume of fcc Fe is much larger than the volume of hcp Fe at pressures below the fcc spin transition pressure ( $\sim 10 \text{ GPa}$ ), but above the fcc spin transition pressure, the volumes of fcc and hcp iron are very similar (Fig. 1b). This makes their elastic properties similar at high- $P$ - $T$  conditions (Martorell et al. 2015). By comparing the spin transition pressure in fcc pure Fe and FeH, we can conclude that the existence of hydrogen in the lattice stabilizes the magnetic properties of fcc Fe to a higher pressure (by  $\sim 30 \text{ GPa}$ ), supporting the conclusion proposed by Gomi et al. (2018) that hydrogen can stabilize the magnetism of iron. The bulk magnetic moments and their spin transition in other Fe-H binaries (e.g.,  $P_4/mmm$ - $\text{Fe}_3\text{H}_3$ ,  $Pm\bar{3}m$ - $\text{FeH}_3$ ,  $C2/m$ - $\text{Fe}_3\text{H}_{11}$ , and  $C2/c$ - $\text{FeH}_6$ ) as a function of pressure are presented in Online Materials<sup>1</sup> Figure S4. In  $\text{Fe}_3\text{H}_3$  phase, the magnetic transition happens at a pressure of  $\sim 60 \text{ GPa}$ , while the other Fe-H phases were found to be always stable in the NM state.

**Equation of state**

The third-order Birch-Murnaghan (BM) equation of state (EOS) was used to fit the static  $P$ - $V$  data for fcc FeH as follows:

$$P(V) = \frac{3K_0}{2} \left[ \left( \frac{V_0}{V} \right)^{\frac{7}{3}} - \left( \frac{V_0}{V} \right)^{\frac{5}{3}} \right] \left\{ 1 + \frac{3}{4}(K' - 4) \left[ \left( \frac{V_0}{V} \right)^{\frac{2}{3}} - 1 \right] \right\} \quad (1)$$

where  $P$  is the pressure,  $V$  is the volume,  $V_0$  is the initial volume,  $K_0$  and  $K'$  are the bulk modulus at ambient pressure and its pressure derivative. The equation of state of fcc FeH is listed in Table 1 and plotted in Figure 2, where the values from the literature are also given as references.

The initial volume  $V_0$  calculated in this study is consistent with previous values reported by Narygina et al. (2011) and Kato et al. (2020), with  $<2\%$  difference. As shown in Figure 2, at the pressure range of  $10$ – $40 \text{ GPa}$ , the compressibility of fcc FeH in the NSR state is consistent with the measurements by Narygina et al. (2011), and it is also compatible with those of Thompson et al. (2018). In this region, the compression behavior is controlled by the high-spin ferromagnetism. Our results show that above the spin transition pressure of  $\sim 40 \text{ GPa}$ , there will be a collapse in volume and compressibility, which is in good agreement with the results of Kato et al. (2020). Narygina et al. (2011) and Thompson et al. (2018) reported linear compressibility with no discontinuity observed for fcc  $\text{FeH}_{x-1}$  across a range of  $0$ – $80 \text{ GPa}$ ; however, there were no spin transitions observed in their measurements. The HS to LS spin transition simulated in this study results in a change to the  $\text{FeH}_x$  compressibility, which will play an important role in the elastic properties. As shown in Figure 3, the HS to LS transition in fcc FeH dramatically increases its elastic modulus and sound velocities. By comparison with previous experimental and computational  $P$ - $V$  curves, the differential behaviors in this study may be due to the different site occupations of hydrogen in the fcc FeH lattice. In this study, our iron hydride structures were obtained from global structure prediction tools, which ensured our structures are stable with the lowest formation energies. Parameters of the third-order Birch-Murnaghan equation of states for our Fe-H binaries are reported in Online Materials<sup>1</sup> Table S2.

**Hydrogen-induced volume expansion**

To correlate the density of the core with iron-containing hydrogen, the volume expansion induced by hydrogen in iron must be known. As outlined in the previous sections the spin

**TABLE 1.** Third-order Birch-Murnaghan equation of state parameters for fcc FeH

	$V_0$ ( $\text{\AA}^3/\text{f.u.}$ )	$K_0$ (GPa)	$K'$	$P$ range (GPa)	Reference
$\text{FeH}_{x-1}$	13.45(3)	99(5)	11.7(5)	12–68	Narygina et al. (2011)
FM FeH	13.5	168	4.5	$<50$	Kato et al. (2020)
	13.25	182	4.1	$<40$	This study
NM FeH	12.3	262	4.2		Kato et al. (2020)
	12.14	262	4.5	0–300	This study
fcc-Fe	12.26	111	5.3	0–24	Tsujino et al. (2013)
	11.97	189	4	0–10	
	10.27	283	4.5	10–300	This study
hcp-Fe	11.23(12)	165(fixed)	4.9(4)	17–197	Dewaele et al. (2006)
	10.15	306	4.3	0–300	Bazhanova et al. (2012)
	10.14	311	4.3	0–300	This study

Note: Values in parentheses represent the error of each parameter from experimental data.

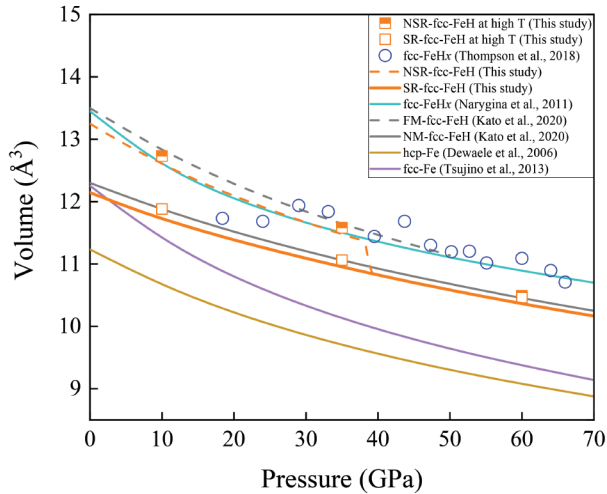


**FIGURE 2.** Compression curves of fcc FeH calculated at 0 K (lines) and along the geothermal temperature (points) in both non-spin-restricted (NSR) and spin-restricted (SR) states. The data sets from the literature are presented for comparison. [blue circle = Thompson et al. (2018), 18–82 GPa, 1500–2000 K; cyan-blue line = Narygina et al. (2011), 12–68 GPa, 300 K; gray line = Kato et al. (2020), both ferromagnetic (FM) and non-magnetic (NM) states at 0 K]. The data of pure hcp Fe (Dewaele et al. 2006, dark yellow line: 17–197 GPa, 300 K) and fcc Fe (Tsujino et al. 2013, purple line: 0–24 GPa, 873–1873 K) are also plotted. (Color online.)

transition induces large changes to this volume expansion and elastic properties even at static conditions. Thus extrapolations of properties across the spin transition are unreliable, and low-pressure measurements of hydrogen-induced volume expansion are likely not to be accurate. Thus we shall calculate this expansion at core relevant pressures and temperatures and use these results from hereon.

In this study, our Fe-H binary structures exhibit that hydrogen occupies the octahedral (O) site, although Ikuta et al. (2019) suggested that a small number of hydrogen atoms could also occupy the tetrahedral (T) site. We infer that this is most likely caused by temperature where the greater configurational entropy of such sites overcomes their enthalpic penalties. The volume expansion in Fe-H binary caused by a single-formula unit of hydrogen,  $\Delta V_{\text{H}}$ , can be determined by:

$$\Delta V_{\text{H}} = \frac{V_{\text{FeH}_x} - V_{\text{Fe}}}{x} \quad (2)$$

where  $V_{\text{FeH}_x}$  and  $V_{\text{Fe}}$  are unit-cell volumes of iron hydride and pure fcc or hcp Fe metal, respectively, and  $x$  is the hydrogen concentration in  $\text{FeH}_x$ .

The calculated volume expansion ( $\Delta V_{\text{H}}$ ) at low  $P$ - $T$  conditions (0–12 GPa, <1200 K) is presented in Figure 4. The data set from previous measurements is also plotted for comparison. The values of  $\Delta V_{\text{H}}$  were calculated to be  $\sim 1.70$  and  $1.94 \text{ \AA}^3$  relative to fcc-Fe and hcp-Fe, respectively. Note that the volumes of pure Fe below 12 GPa were calculated from the experimental EOS (Dewaele et al. 2006; Tsujino et al. 2013) since theoretical absolute densities suffer from small but non-negligible systematic errors of theory at low pressure (see Online Materials' Fig. S5–S6). Our predicted

$\Delta V_{\text{H}}$  values are smaller than the experimental value of  $2.22 \text{ \AA}^3$  reported by Ikuta et al. (2019) but are compatible with those of other 3d-transition metal hydrides (i.e.,  $\epsilon\text{-MnH}_{x>0.6}$ :  $1.66 \text{ \AA}^3$ ,  $\epsilon\text{-CoH}_{x<0.6}$ :  $1.8 \text{ \AA}^3$ ) (Fukai 2005), and our results are also similar to the experimental value of  $\sim 1.90 \text{ \AA}^3$  reported by Sakamaki et al. (2009). We confirmed that the volume expansion is approximately linear under low pressures (0–12 GPa), consistent with the findings of Ikuta et al. (2019). However, in the whole Earth pressure range, the volume expansion is no longer linear as it collapses at  $\sim 40$  GPa due to the iron HS to LS spin transition after which a new linear regime is obtained, as shown in Figure 5. This is consistent with the results proposed by Gomi et al. (2018), as they observed a decrease in volume attributed to the magnetic transition in hcp FeH.

Volume expansion of all considered Fe-H binaries at core  $P$ - $T$

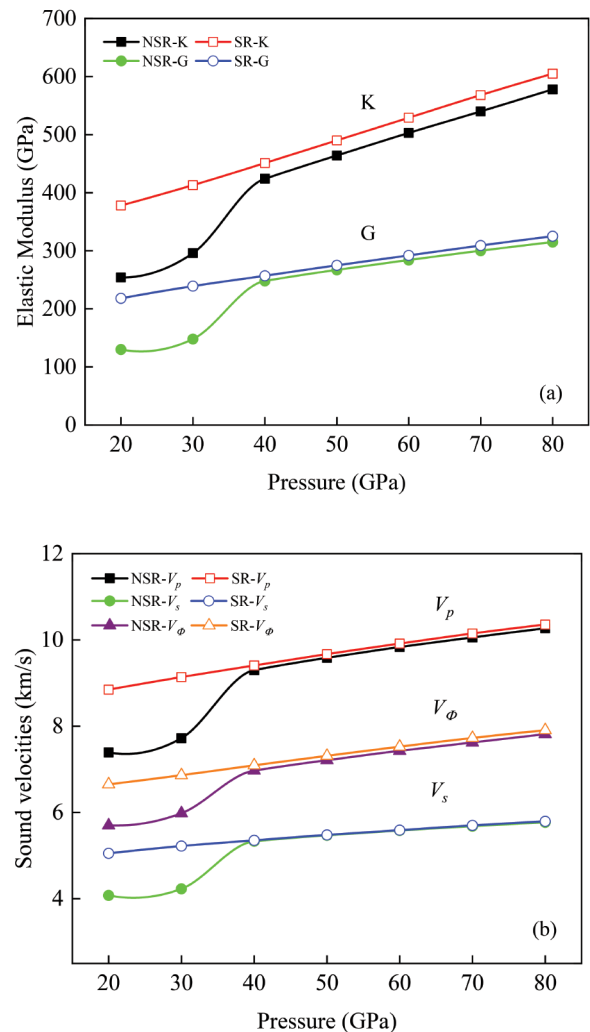


**FIGURE 3.** Seismic properties of fcc FeH at the HS to LS transition pressure range. (a) bulk modulus ( $K$ ) and shear modulus ( $G$ ); (b) sound velocities ( $V_p$ ,  $V_s$ , and  $V_\phi$ ). In a and b, the straight lines represent the SR states while the curves represent the NSR states of fcc FeH. The spin transition in fcc FeH dramatically increases its elastic modulus and sound velocities. (Color online.)

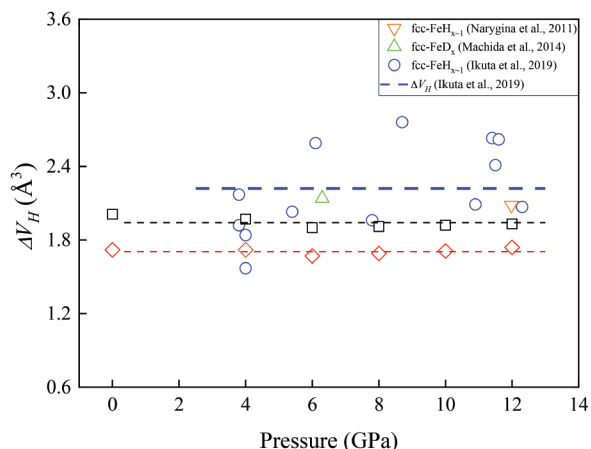


**FIGURE 4.** Hydrogen induced FeH volume expansion at low temperatures (<1200 K) and pressures (0–12 GPa). The black squares and red cubes are relative to the volume of hcp-Fe and fcc-Fe, respectively. Blue circles and the orange lower triangle are the experimental results determined by Ikuta et al. (2019) and Narygina et al. (2011), respectively. The green upper triangle is iron deuteride (FeD<sub>x</sub>) at 6.3 GPa and 988 K determined by Machida et al. (2014). The dashed lines are the linear fit to the data points. (Color online.)

conditions (300–380 GPa, ~5000 K) are presented in Figure 6. We have plotted the volume expansion with respect to fcc-Fe (Fig. 6a) and hcp-Fe (Fig. 6b), respectively. The  $\Delta V_H$  in fcc FeH was calculated as ~1.07 Å<sup>3</sup> at the Earth’s inner core *P-T* conditions. This is considerably smaller than the numbers obtained at low-*P-T* conditions. Thus using values  $\Delta V_H$  obtained at low-*P-T* conditions will severely underestimate the amount of hydrogen in the Earth’s core. These underestimates are mostly due to the low-*P* values, which neglect the spin transition, but a low *T* also

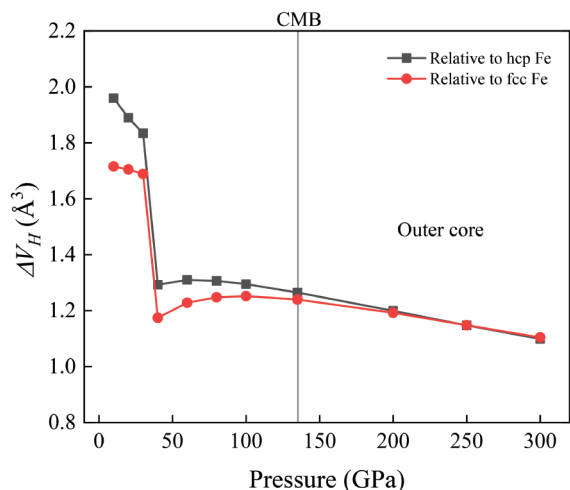


**FIGURE 5.** Hydrogen induced FeH volume expansion at the pressure range of 10–300 GPa. The black squares and red circles represent the results calculated relative to  $V_{\text{fcc-Fe}}$  and  $V_{\text{hcp-Fe}}$ , respectively.  $V_{\text{fcc-Fe}}$  and  $V_{\text{hcp-Fe}}$  are calculated from the equation of state of fcc Fe (Tsujino et al. 2013) and hcp Fe (Dewaele et al. 2006), respectively. The Fe spin transition in FeH induced volume expansion collapse at the pressure of ~40 GPa. (Color online.)

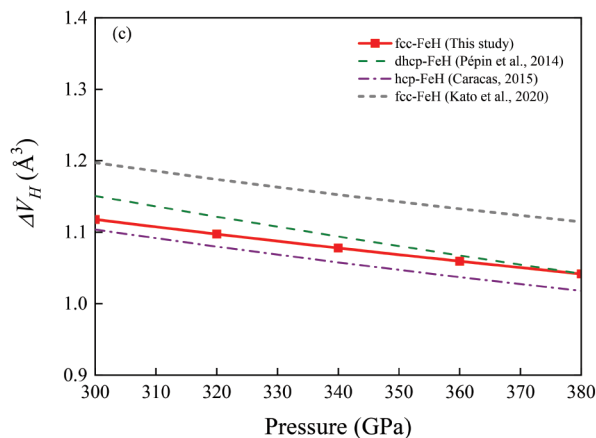
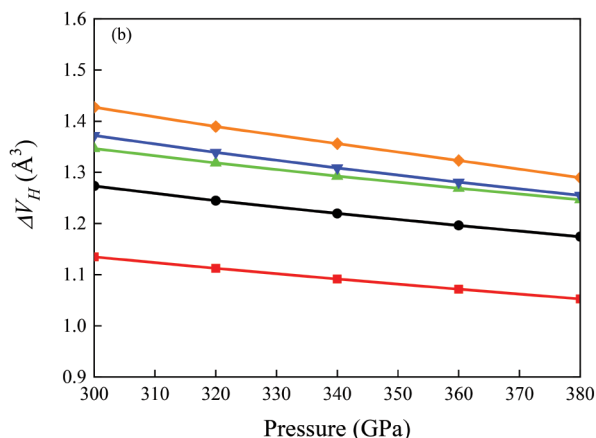
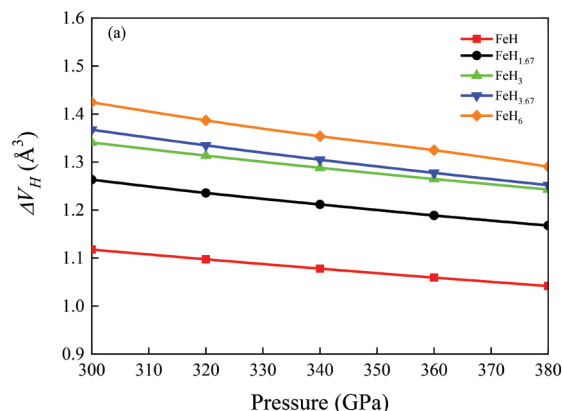


**FIGURE 6.** Hydrogen induced volume expansion in Fe-H binaries at Earth’s core *P-T* conditions (300–380 GPa, ~5000 K) in relative to fcc-Fe (a) and hcp-Fe (b). The literature data relative to fcc-Fe at ambient temperature conditions are plotted for comparison (c). (Color online.)

affects the results. At static conditions with inner core *P* values, we predict  $\Delta V_H$  to be ~1.10 Å<sup>3</sup>, and thus both *P* and *T* must be accurately represented in estimates of the volume expansion.

In Figure 6c, we show previous estimates of volume expansion taken from the literature of fcc FeH (Kato et al. 2020), hcp FeH (Caracas 2015), and dhcp FeH (Pépin et al. 2014) at ambient temperature (300 K). They reported volume expansion values

of  $\sim 1.06\text{--}1.15 \text{ \AA}^3$ , which are slightly higher or lower than those determined in our calculation. The various crystal structures of FeH alloy, extrapolation error of data from low temperature, and the different site occupancies of hydrogen in FeH lattice may account for these volume expansion differences. Since our values are determined with the most stable FeH lattice and at the correct temperature, we shall use our core  $P\text{-}T \Delta V_{\text{H}}$  values to estimate hydrogen contents.

### IMPLICATIONS

The Earth's core is mainly composed of a Fe-Ni alloy along with a few percent of light elements, such as Si, C, O, S, N, and H required to explain its density deficit and seismic properties (Birch 1952). The outer and inner core are  $\sim 5\text{--}10\%$  and  $\sim 1\text{--}2\%$  less dense, respectively, than pure iron at relevant temperature and pressure conditions (Anderson and Isaak 2002; Shearer and Masters 1990; Stixrude et al. 1997). Hydrogen is the most abundant element in the solar system, and therefore, it is plausibly one of the main light element candidates in the Earth's core. The solubility of hydrogen in iron increases considerably with pressure (Fukai 1984; Ohtani et al. 2005; Okuchi 1997). Based on high-temperature and high-pressure in situ neutron diffraction experiments, Iizukaoku et al. (2017) proposed that iron preferentially incorporates hydrogen, which may affect other light elements partitioning into the core in the later processes.

The hydrogen content in the Earth's core has been previously estimated (Ikuta et al. 2019; Narygina et al. 2011; Thompson et al. 2018) by comparing the volume expansion and density deficits introduced by hydrogen in the Fe lattice with the profile of PREM (Dziewonski and Anderson 1981). However, in those previous studies, the volume expansion  $\Delta V_{\text{H}}$  was obtained at low-pressure conditions and was extrapolated linearly to high pressure to calculate the hydrogen content in the Earth's core. As we have discussed above, due to a volume collapse caused by the iron spin transition, the hydrogen-driven volume expansion ( $\Delta V_{\text{H}}$ ) of Fe at high pressure has a much lower value ( $\sim 30\%$  less) than it does at lower pressures. Therefore, we conclude that the previous works which used a high value of  $\Delta V_{\text{H}}$  might underestimate the H content of the Earth's core.

We re-examined the hydrogen content in the Earth's core using our updated volume expansion ( $\Delta V_{\text{H}}$ ) determined at the Earth's core conditions (135 GPa and 4000 K for the CMB and 330 GPa and 5000 K for the ICB). The results are given in Table 2, where the results of previous studies are also listed for comparison. Using these methods, we estimate a hydrogen content of the outer core of  $\sim 0.54\text{--}1.10 \text{ wt}\%$  (equal to  $15.07 \pm 5.15 \times 10^{21} \text{ kg}$ ). Umemoto and Hirose (2015) previously examined the hydrogen content of the outer core by constraining both density and sound velocities. They suggested that liquid Fe with  $\sim 1 \text{ wt}\%$  hydrogen could satisfy the seismic properties of the outer core, which is exactly within the range of our estimated value. This hydrogen content stored in the outer core would be equivalent to  $97 \pm 33$  times the mass of liquid water in the ocean.

Figure 7 plots the hydrogen contents required to meet the inner core density deficit ( $1\text{--}2\%$ ) as in all considered  $\text{FeH}_x$  binaries (e.g.,  $Fm\bar{3}m\text{-FeH}$ ,  $P_4/mmm\text{-Fe}_3\text{H}_5$ ,  $Pm\bar{3}m\text{-FeH}_3$ ,  $C2/m\text{-Fe}_3\text{H}_{11}$ , and  $C2/c\text{-FeH}_6$ ), with respect to both fcc and hcp Fe. To estimate the average hydrogen content in the combination of

**TABLE 2.** Hydrogen content in the Earth's core based on the volume expansion of fcc  $\text{FeH}_x$

$\Delta V_{\text{H}}$ ( $\text{\AA}^3$ )	Hydrogen content (wt%)		Reference
	Outer core	Inner core	
	<b>Relative to fcc-Fe</b>		
1.45*/(1.05)	0.80–1.10	0.20–0.30	Thompson et al. (2018)
2.22	0.40–0.90	0.07–0.17	Ikuta et al. (2019)
1.37*/(1.06)	0.55–1.10	0.10–0.22	This study
	<b>Relative to hcp-Fe</b>		
1.90	0.50–1.00	0.08–0.16	Narygina et al. (2011)
1.39*/(1.07)	0.54–1.08	0.10–0.20	This study

Notes: The values with asterisk represent the volume expansion for the CBM, while values in parentheses are for the ICB.

these  $\text{FeH}_x$  phases, we adopted their phase distribution probability results with an ideal mixture of 30% of fcc FeH, 22% of each  $\text{Fe}_3\text{H}_5$  and  $\text{Fe}_3\text{H}_{11}$ , 11% of  $\text{FeH}_3$ , and 15% of  $\text{FeH}_6$  (see Online Materials<sup>1</sup> Table S3). The average hydrogen content in the Earth's inner core is then estimated to be  $\sim 0.10\text{--}0.22 \text{ wt}\%$  (equal to  $0.16 \pm 0.6 \times 10^{21} \text{ kg}$ ). Although the solid inner core, at the center of the wide iron ocean, represents only 4.3% of the volume of the core and  $<1\%$  of the volume of the Earth, its maximum hydrogen content could be equivalent to  $1.0 \pm 0.4$  times the mass of liquid water in the ocean.

Determination of the temperature of hydrogen-bearing Earth's core is essential for understanding its thermal evolution. Sakamaki et al. (2009) and Hirose et al. (2019) have reported that the melting temperature of Fe-H alloys under CMB pressure is  $\sim 2380\text{--}2600 \text{ K}$ , lower than that of Fe alloyed with the other possible core light elements though its melting temperature at inner core pressure conditions has not yet been well determined. By using the Simon-Glatzel equation,  $T_{\text{melting}} = T_0 [(P_{\text{melting}} - P_0)/a + 1]^{1/c}$ ,  $a = 24.6$ ,  $c = 3.8$ ,  $T_0 = 1473 \text{ K}$ , and  $P_0 = 9.5 \text{ GPa}$  (Sakamaki et al. 2009), these melting temperatures can be extrapolated to higher pressures. This gives a melting temperature of FeH

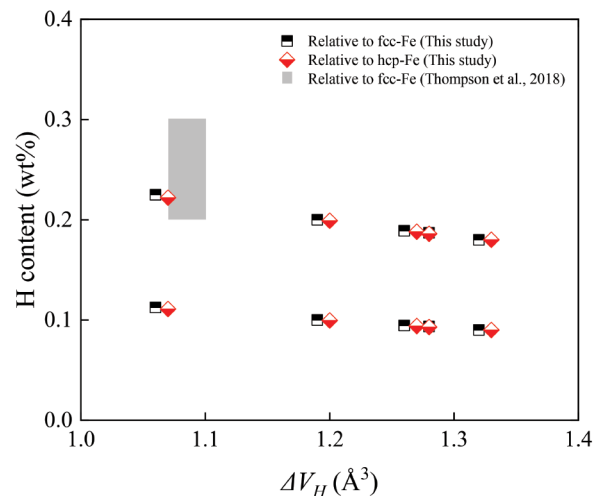


**FIGURE 7.** Hydrogen content in the Earth's inner core as a function of volume expansion relative to both fcc-Fe (black square) and hcp-Fe (red cube). The varied values of volume expansion are determined by different Fe-H binaries (Fig. 6). The gray area ( $0.2\text{--}0.3 \text{ wt}\%$  hydrogen content) was estimated by Thompson et al. (2018). According to the calculated Fe-H binaries phase distribution and the density deficit of the inner core ( $\sim 1\text{--}2\%$ ), the hydrogen content in the inner core is estimated to be  $\sim 0.10\text{--}0.22 \text{ wt}\%$ . (Color online.)



(~1.77 wt% H) at ICB pressure (~330 GPa) ~2950 K. The melting temperature of pure iron at ICB pressure has been estimated to be ~6200 K (Alfè 2009; Sun et al. 2018). The melting temperature of a real hydrous core is predicted to be between these two temperatures as hydrogen will depress the melting temperature from pure iron, but the estimation of FeH melting temperature is too low as its hydrogen content is much higher than we predict for the core. The CMB temperature is estimated to be ~4550 K from the adiabatic temperature gradient (Gomi et al. 2018). A linear extrapolation of the effect of hydrogen would give a melting temperature of hydrogen-bearing components in the ICB and CMB as  $\sim 5900 \pm 100$  K and  $\sim 3650 \pm 300$  K, respectively (see color regions in Fig. 8). These results indicate that hydrogen would induce a relatively low core temperature. The temperature of hydrogen-bearing ICB is ~300 K lower than that of pure iron, and the CMB temperature is ~500 K colder than the previous estimation ( $\sim 4150 \pm 250$  K) by Boehler (1993, 1996).

Note that a linear relationship of melting temperature with hydrogen would require that the variation of free energy with hydrogen should be the same in the solid and the liquid. However, this will not be the case. The width of this phase loop will, in part, define the nonlinearity. As the partitioning of hydrogen between the two phases is not particularly strong (Okuchi 1997), this phase loop will necessarily be narrow, and thus deviations from linearity as varied partitioning will not be strong. The error involved in extrapolating the FeH melting temperature to higher pressures limits the ability to constrain this melting temperature further with more detailed consideration of the partitioning, but the partitioning of hydrogen to the liquid phase will likely lower the actual melting temperature somewhat.

The density deficit in the core is a crucial consideration for geochemical models of the core composition. Other light elements (e.g., Si, O, S, N, and C) will also play an essential role in the volume expansion, which needs to be addressed in future studies. However, the presence of Ni at Earth's core  $P$ - $T$  condi-

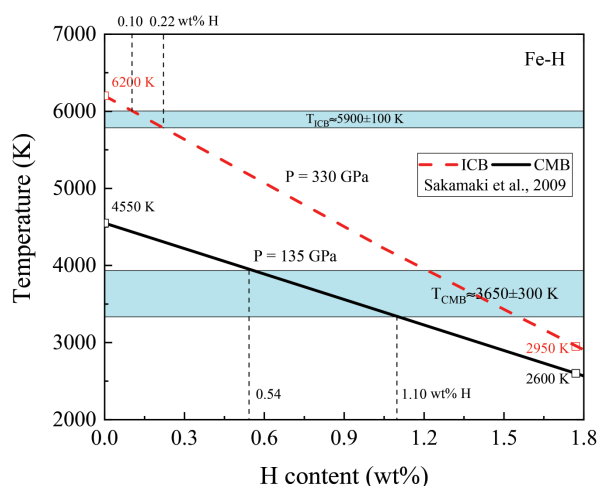


**FIGURE 8.** The melting temperatures of hydrogen-bearing ICB (red line) and CMB (black line) as a function of H content. The dash vertical lines represent the H content in our calculations, and the corresponding temperatures of hydrogen-bearing ICB and CMB are shown by the color regions. (Color online.)

tions does not noticeably change the density deficits from pure iron (Anderson and Isaak 2002; Martorell et al. 2013) though it may impact on the properties of hydrogen-containing iron by changing the properties of the interstitial sites where hydrogen resides. It is worth pointing out that the elastic properties of the core are another constraint on estimating its composition. Only by comparison and matching with both density and elastic models of the Earth's core can we estimate precisely the composition of the core, which might be a mixture of iron with several light elements, including hydrogen. On the other hand, the density deficit of the core is still an unsolved problem. In this study, we demonstrated that higher amounts of hydrogen are needed to resolve this problem than previously predicted. Other light elements may change this story somewhat, and the presence of all elements needs to be considered simultaneously, especially at the temperature and pressure conditions of the core.

## ACKNOWLEDGMENTS

We thank two anonymous reviewers for their constructive comments and suggestions, which greatly improved the quality of the manuscript. H.Y. thanks Prof. Yunguo Li for his fruitful discussions.

## FUNDING

This work was supported by the National Natural Science Foundation of China (41773057, 42050410319) and Science and Technology Foundation of Guizhou Province (ZK2021-205), with computational resources from Computer Simulation Labs of IGGCAS, the National Supercomputer Center in Shenzhen, the TH-2 High-Performance Computer System in Lvliang, China.

## REFERENCES CITED

- Alfè, D. (2009) PHON: A program to calculate phonons using the small displacement method. *Computer Physics Communications*, 180, 2622–2633, <https://doi.org/10.1016/j.cpc.2009.03.010>.
- Alfè, D., Price, G., and Gillan, M. (2001) Thermodynamics of hexagonal-close-packed iron under Earth's core conditions. *Physical Review B: Condensed Matter*, 64, 045123, <https://doi.org/10.1103/PhysRevB.64.045123>.
- Allègre, C.J., Poirier, J.P., Humler, E., and Hofmann, A.W. (1995) The chemical composition of the Earth. *Earth and Planetary Science Letters*, 134, 515–526, [https://doi.org/10.1016/0012-821X\(95\)00123-T](https://doi.org/10.1016/0012-821X(95)00123-T).
- Anderson, O.L. and Isaak, D.G. (2002) Another look at the core density deficit of Earth's outer core. *Physics of the Earth and Planetary Interiors*, 131, 19–27, [https://doi.org/10.1016/S0031-9201\(02\)00017-1](https://doi.org/10.1016/S0031-9201(02)00017-1).
- Bazhanova, Z.G., Oganov, A.R., and Gianola, O. (2012) Fe-C and Fe-H systems at pressures of the Earth's inner core. *Physics Uspekhi*, 55, 489–497, <https://doi.org/10.3367/UFNe.0182.201205c.0521>.
- Birch, F. (1952) Elasticity and constitution of the Earth's interior. *Journal of Geophysical Research*, 57, 227–286, <https://doi.org/10.1029/JZ057i002p00227>.
- Blöchl, P.E. (1994) Projector augmented-wave method. *Physical Review B: Condensed Matter*, 50, 17953–17979, <https://doi.org/10.1103/PhysRevB.50.17953>.
- Boehler, R. (1993) Temperatures in the Earth's core from melting-point measurements of iron at high static pressures. *Nature*, 363, 534–536, <https://doi.org/10.1038/363534a0>.
- (1996) Experimental constraints on melting conditions relevant to core formation. *Geochimica et Cosmochimica Acta*, 60, 1109–1112, [https://doi.org/10.1016/0016-7037\(96\)00021-X](https://doi.org/10.1016/0016-7037(96)00021-X).
- Caracas, R. (2015) The influence of hydrogen on the seismic properties of solid iron. *Geophysical Research Letters*, 42, 3780–3785, <https://doi.org/10.1002/2015GL063478>.
- Dewaele, A., Loubeyre, P., Occelli, F., Mezouar, M., Dorogokupets, P.I., and Torrent, M. (2006) Quasihydrostatic equation of state of iron above 2 Mbar. *Physical Review Letters*, 97, 215504, <https://doi.org/10.1103/PhysRevLett.97.215504>.
- Dziewonski, A.M. and Anderson, D.L. (1981) Preliminary reference Earth model. *Physics of the Earth and Planetary Interiors*, 25, 297–356, [https://doi.org/10.1016/0031-9201\(81\)90046-7](https://doi.org/10.1016/0031-9201(81)90046-7).
- Elsässer, C., Zhu, J., Louie, S., Meyer, B., Fähnle, M., and Chan, C. (1998) Ab initio study of iron and iron hydride: II. Structural and magnetic properties of close-packed Fe and FeH. *Journal of Physics Condensed Matter*, 10, 5113–5129, <https://doi.org/10.1088/0953-8984/10/23/013>.
- Fukai, Y. (1984) The iron-water reaction and the evolution of the Earth. *Nature*, 308, 174–175, <https://doi.org/10.1038/308174a0>.
- (2005) *The Metal-Hydrogen System: Basic Bulk Properties*, 2nd edition,

- 500 p. Chapter 4, Springer.
- Gomi, H., Fei, Y., and Yoshino, T. (2018) The effects of ferromagnetism and interstitial hydrogen on the equation of states of hcp and dhcp FeH<sub>x</sub>: Implications for the Earth's inner core age. *American Mineralogist*, 103, 1271–1281, <https://doi.org/10.2138/am-2018-6295>.
- Hirose, K., Tagawa, S., Kuwayama, Y., Sinmyo, R., Morard, G., Ohishi, Y., and Genda, H. (2019) Hydrogen limits carbon in liquid iron. *Geophysical Research Letters*, 46, 5190–5197, <https://doi.org/10.1029/2019GL082591>.
- Iizuka-Oku, R., Yagi, T., Gotou, H., Okuchi, T., Hattori, T., and Sano-Furukawa, A. (2017) Hydrogenation of iron in the early stage of Earth's evolution. *Nature Communications*, 8, 14096, <https://doi.org/10.1038/ncomms14096>.
- Ikuta, D., Ohtani, E., Sano-Furukawa, A., Shibazaki, Y., Terasaki, H., Yuan, L., and Hattori, T. (2019) Interstitial hydrogen atoms in face-centered cubic iron in the Earth's core. *Scientific Reports*, 9, 7108, <https://doi.org/10.1038/s41598-019-43601-z>.
- Karki, B.B., Stixrude, L., and Wentzcovitch, R.M. (2001) High-pressure elastic properties of major materials of Earth's mantle from first principles. *Reviews of Geophysics*, 39, 507–534, <https://doi.org/10.1029/2000RG000088>.
- Kato, C., Umemoto, K., Ohta, K., Tagawa, S., Hirose, K., and Ohishi, Y. (2020) Stability of fcc phase FeH to 137 GPa. *American Mineralogist*, 105, 917–921, <https://doi.org/10.2138/am-2020-7153>.
- Kohn, W. and Sham, L.J. (1965) Self-consistent equations including exchange and correlation effects. *Physical Review*, 140 (4A), A1133–A1138, <https://doi.org/10.1103/PhysRev.140.A1133>.
- Kresse, G. and Furthmüller, J. (1996) Efficient iterative schemes for ab initio total-energy calculations using a plane-wave basis set. *Physical Review B*, 54, 11169, <https://doi.org/10.1103/PhysRevB.54.11169>.
- Lyakhov, A.O., Oganov, A.R., Stokes, H.T., and Zhu, Q. (2013) New developments in evolutionary structure prediction algorithm USPEX. *Computer Physics Communications*, 184, 1172–1182, <https://doi.org/10.1016/j.cpc.2012.12.009>.
- Machida, A., Saitoh, H., Sugimoto, H., Hattori, T., Sano-Furukawa, A., Endo, N., Katayama, Y., Iizuka, R., Sato, T., Matsuo, M., and others. (2014) Site occupancy of interstitial deuterium atoms in face-centred cubic iron. *Nature Communications*, 5, 5063, <https://doi.org/10.1038/ncomms6063>.
- Martorell, B., Brodholt, J., Wood, I.G., and Vočadlo, L. (2013) The effect of nickel on the properties of iron at the conditions of Earth's inner core: Ab initio calculations of seismic wave velocities of Fe-Ni alloys. *Earth and Planetary Science Letters*, 365, 143–151, <https://doi.org/10.1016/j.epsl.2013.01.007>.
- (2015) The elastic properties and stability of fcc-Fe and fcc-FeNi alloys at inner-core conditions. *Geophysical Journal International*, 202, 94–101, <https://doi.org/10.1093/gji/ggv128>.
- Monkhorst, H.J. and Pack, J.D. (1976) Special points for Brillouin-zone integrations. *Physical Review B, Solid State*, 13, 5188–5192, <https://doi.org/10.1103/PhysRevB.13.5188>.
- Narygina, O., Dubrovinsky, L.S., McCammon, C.A., Kurnosov, A., Kantor, I.Y., Prakapenka, V.B., and Dubrovinskaja, N.A. (2011) X-ray diffraction and Mössbauer spectroscopy study of fcc iron hydride FeH at high pressures and implications for the composition of the Earth's core. *Earth and Planetary Science Letters*, 307, 409–414, <https://doi.org/10.1016/j.epsl.2011.05.015>.
- Nosé, S. (1984) A molecular-dynamics method for simulations in the canonical ensemble. *Molecular Physics*, 52, 255–268, <https://doi.org/10.1080/00268978400101201>.
- Oganov, A.R., Lyakhov, A.O., and Valle, M. (2011) How evolutionary crystal structure prediction works—And why. *Accounts of Chemical Research*, 44, 227–237, <https://doi.org/10.1021/ar1001318>.
- Ohtani, E., Hirao, N., Kondo, T., Ito, M., and Kikogawa, T. (2005) Iron-water reaction at high pressure and temperature, and hydrogen transport into the core. *Physics and Chemistry of Minerals*, 32, 77–82, <https://doi.org/10.1007/s00269-004-0443-6>.
- Okuchi, T. (1997) Hydrogen partitioning into molten iron at high pressure: Implications for Earth's core. *Science*, 278, 1781–1784, <https://doi.org/10.1126/science.278.5344.1781>.
- Pépin, C.M., Dewaele, A., Geneste, G., Loubeyre, P., and Mezouar, M. (2014) New iron hydrides under high pressure. *Physical Review Letters*, 113, 265504, <https://doi.org/10.1103/PhysRevLett.113.265504>.
- Perdew, J.P., Burke, K., and Ernzerhof, M. (1996) Generalized gradient approximation made simple. *Physical Review Letters*, 77, 3865–3868, <https://doi.org/10.1103/PhysRevLett.77.3865>.
- Poirier, J.P. (1994) Light elements in the Earth's outer core: A critical review. *Physics of the Earth and Planetary Interiors*, 85, 319–337, [https://doi.org/10.1016/0031-9201\(94\)90120-1](https://doi.org/10.1016/0031-9201(94)90120-1).
- Ringwood, A.E. (1984) The Earth's core - Its composition, formation and bearing upon the origin of the Earth (The Bakerian Lecture 1983). *Proceedings of the Royal Society A Mathematical Physical and Engineering Sciences*, 395, 1–46.
- Sakamaki, K., Takahashi, E., Nakajima, Y., Nishihara, Y., Funakoshi, K., Suzuki, T., and Fukai, Y. (2009) Melting phase relation of FeH<sub>x</sub> up to 20 GPa: Implication for the temperature of the Earth's core. *Physics of the Earth and Planetary Interiors*, 174, 192–201, <https://doi.org/10.1016/j.pepi.2008.05.017>.
- Shearer, P. and Masters, G. (1990) The density and shear velocity contrast at the inner core boundary. *Geophysical Journal International*, 102, 491–498, <https://doi.org/10.1111/j.1365-246X.1990.tb04481.x>.
- Söderlind, P., Moriarty, J.A., and Wills, J.M. (1996) First-principles theory of iron up to earth-core pressures: Structural, vibrational, and elastic properties. *Physical Review B: Condensed Matter*, 53, 14063–14072, <https://doi.org/10.1103/PhysRevB.53.14063>.
- Stixrude, L., Wasserman, E., and Cohen, R.E. (1997) Composition and temperature of Earth's inner core. *Journal of Geophysical Research*, 102 (B11), 24729–24739, <https://doi.org/10.1029/97JB02125>.
- Sun, T., Brodholt, J.P., Li, Y., and Vočadlo, L. (2018) Melting properties from ab initio free energy calculations: Iron at the Earth's inner-core boundary. *Physical Review B*, 98, 224301, <https://doi.org/10.1103/PhysRevB.98.224301>.
- Thompson, E.C., Davis, A.H., Bi, W., Zhao, J., Alp, E.E., Zhang, D., Greenberg, E., Prakapenka, V.B., and Campbell, A.J. (2018) High-pressure geophysical properties of fcc phase FeH<sub>x</sub>. *Geochemistry, Geophysics, Geosystems*, 19, 305–314, <https://doi.org/10.1002/2017GC007168>.
- Togo, A., Oba, F., and Tanaka, I. (2008) First-principles calculations of the ferroelastic transition between rutile-type and CaCl<sub>2</sub>-type SiO<sub>2</sub> at high pressures. *Physical Review B: Condensed Matter and Materials Physics*, 78, 134106, <https://doi.org/10.1103/PhysRevB.78.134106>.
- Tsujino, N., Nishihara, Y., Nakajima, Y., Takahashi, E., Funakoshi, K.I., and Higo, Y. (2013) Equation of state of γ-Fe: Reference density for planetary cores. *Earth and Planetary Science Letters*, 375, 244–253, <https://doi.org/10.1016/j.epsl.2013.05.040>.
- Umemoto, K. and Hirose, K. (2015) Liquid iron-hydrogen alloys at outer core conditions by first-principles calculations. *Geophysical Research Letters*, 42, 7513–7520, <https://doi.org/10.1002/2015GL065899>.
- Vočadlo, L., Brodholt, J., Dobson, D.P., Knight, K.S., Marshall, W.G., Price, G.D., and Wood, I.G. (2002) The effect of ferromagnetism on the equation of state of Fe<sub>3</sub>C studied by first-principles calculations. *Earth and Planetary Science Letters*, 203, 567–575, [https://doi.org/10.1016/S0012-821X\(02\)00839-7](https://doi.org/10.1016/S0012-821X(02)00839-7).

MANUSCRIPT RECEIVED JULY 31, 2021

MANUSCRIPT ACCEPTED MAY 6, 2022

ACCEPTED MANUSCRIPT ONLINE MAY 18, 2022

MANUSCRIPT HANDLED BY MAINAK MOOKHERJEE

## Endnote:

<sup>1</sup>Deposit item AM-23-48237, Online Materials. Deposit items are free to all readers and found on the MSA website, via the specific issue's Table of Contents (go to [http://www.minsocam.org/MSA/AmMin/TOC/2023/Apr2023\\_data/Apr2023\\_data.html](http://www.minsocam.org/MSA/AmMin/TOC/2023/Apr2023_data/Apr2023_data.html)).